ISSN: 2347-467X, Vol. 14, No. (1) 2026, Pg. 371-382

Current Research in Nutrition and Food Science

www.foodandnutritionjournal.org

Evaluation of the Impact of Solar Exposure on Soluble Solids, Fractal Dimension, and Colorimetry in Oca (*Oxalis Tuberosa* L.) Under High Altitude Conditions

EDWARD TORRES-CRUZ[1], SAIRE ROENFI GUERRA LIMA[1]*, FRED TORRES-CRUZ[2], WENCESLAO TEDDY MEDINA ESPINOZA[1] and NURY YANETH MAYTA-BARRIOS[1]

[1]Academic Department of Agroindustrial Engineering, Universidad Nacional del Altiplano de Puno, Puno, Peru.
[2]Academic Department of Statistics and Informatics Engineering, Universidad Nacional del Altiplano de Puno, Puno, Peru.

Abstract

Oca (*Oxalis tuberosa* L.) is an Andean tuber traditionally sun-cured to enhance sweetness and sensory quality; however, quantitative evidence linking changes in total soluble solids (°Brix) with physical and colorimetric modifications remains limited. This study evaluated the effect of a 10-hour sun-curing process on four oca varieties by monitoring total soluble solids (°Brix), fractal dimension, and color attributes. Measurements were recorded every two hours during the sun-curing period and analyzed both individually and within a consolidated dataset. Results showed a consistent increase in total soluble solids (°Brix) across all varieties, with a strong positive correlation between °Brix values and sun-curing time (r = 0.88–0.94). Total soluble solids were strongly associated with fractal dimension and exhibited moderate-to-strong, variety-dependent correlations with color variation (r = 0.76–0.85), indicating that microstructural and chromatic changes accompany increases in °Brix during solar exposure. In contrast, tuber size parameters showed weak, non-significant correlations with °Brix (r < 0.30), suggesting that physical dimensions have limited influence on soluble solid accumulation. Overall, the consolidated analysis confirmed comparably consistent trends among varieties. These findings demonstrate that integrating physicochemical, fractal, and color-based indicators provides a robust approach for evaluating sun-curing effectiveness and postharvest quality in oca.

Article History
Received: 13 January 2026
Accepted: 10 March 2026

Keywords
°Brix;
Colorimetric Analysis;
Df Fractal Dimension;
Image Processing;
Oxalis Tuberosa L.;
Sun-Curing.

CONTACT Saire Roenfi Guerra Lima srguerr@unap.edu.pe Academic Department of Agroindustrial Engineering, Universidad Nacional del Altiplano de Puno, Puno, Peru.

Doi: http://dx.doi.org/10.12944/CRNFSJ.14.1.25

Introduction

Oca (*Oxalis tuberosa* L.) is a tuber native to the Andean region of South America, traditionally cultivated in high-altitude areas. Its high tolerance to harsh climatic conditions and poor soils allows it to grow where many other crops cannot.[1,2] For this reason, oca is a key staple food and an important contributor to food security for millions of people in the Andes.[3–5] Andean farmers have long applied a traditional practice of exposing harvested tubers to sunlight to reduce bitterness and enhance perceived sweetness. Sun exposure induces metabolic changes, including starch hydrolysis and reductions in oxalic acid content.[6,7] Although these biochemical changes have been described, the associated physical and structural surface modifications occurring during solar exposure remain insufficiently quantified using objective computational approaches.[8–12] During sun-curing, the tuber progressively loses moisture and turgor pressure, resulting in epidermal contraction and surface remodeling.[13–16] However, the relationship between these morphological changes and variations in total soluble solids has not been clearly established, particularly across different oca varieties.

This study employs Fractal Dimension as a non-invasive metric to characterize the evolution of surface morphological complexity as a function of exposure time.[17–20] As dehydration progresses, mechanical stress alters the tuber's epidermal structure.[21–24] These geometric transformations may provide a measurable structural signature associated with internal physiological processes.[25–29] Through digital image processing techniques, fractal analysis enables standardized numerical quantification of surface irregularities beyond subjective visual assessment.[30–32] Simultaneously, total soluble solids, expressed as the °Brix index, serve as the primary physicochemical indicator of changes occurring during sun-curing.[6,33] The rate of carbohydrate transformation is influenced by the duration and intensity of solar radiation.[13,34,35] Nevertheless, the temporal relationship between exposure time, total soluble solids, and surface morphological evolution remains poorly characterized.[36–38] Clarifying this interaction is essential for optimizing postharvest management strategies and improving consistency in organoleptic quality for agro-industrial applications.[39,40] This study tested the hypothesis that surface morphological complexity, quantified through fractal dimension, is associated with variations in total soluble solids (°Brix) during traditional sun-curing of four oca varieties.[41–43]

The objective of the present research was to evaluate the relationship between total soluble solids (°Brix) and surface modifications of oca tubers during a controlled sun-curing process, using digital image analysis to quantify fractal dimension and color variation. By monitoring tubers over defined exposure intervals, we aimed to determine whether fractal dimension can function as a reliable morphological indicator of changes in total soluble solids and whether this relationship differs among varieties. Establishing such associations would provide an objective analytical framework to support scientific characterization of traditional sun-curing practices and contribute to improved quality control in Andean tuber production systems

Materials and Methods

Plant Material and Experimental Site

Four ecotypes of Andean oca (*Oxalis tuberosa* L.) were evaluated, selected based on pigmentation diversity and relevance in traditional post-harvest practices.[44,45] The varieties included: (i) Oca INIA 407 K'eny Roja Molina–Salcedo; (ii) Oca K'eny Roja Sicuani–Cusco; (iii) Oca K'eny Amarilla Capachica; and (iv) Oca K'eny Amarilla Yunguyo. Tubers were harvested at physiological maturity and manually sorted to ensure uniform size, absence of visible mechanical damage, and similar physiological age. Five biological replicates per variety were used. The experiment was conducted in the highlands of Puno, Peru (>3,800 m a.s.l.), under environmental conditions representative of traditional Andean sun-curing practices.[45]

Sun-Curing Procedure

Traditional sun-curing was reproduced under natural field conditions. Tubers were placed outdoors on clean surfaces and exposed to direct solar radiation for 10 continuous hours (08:00–18:00 local time). To ensure uniform exposure, tubers were manually rotated every two hours to prevent shading effects.[33] Measurements were performed at 0, 2, 4, 6, 8, and 10 hours of exposure.

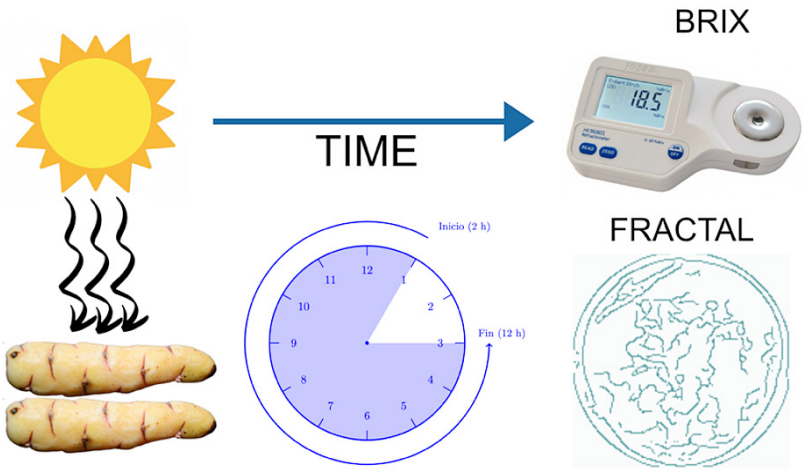

Fig. 1: Solar curing dynamics: brix and fractal analysis

Measurement of Total Soluble Solids (°Brix)
Total soluble solids (TSS) were determined using a digital refractometer (Hanna HI 96811) equipped with Automatic Temperature Compensation (ATC). For each replicate:

- Tubers were longitudinally sectioned.
- Juice was mechanically extracted using manual compression.
- A drop of homogenized juice was placed on the prism surface.
- The prism was cleaned and dried between measurements.

The instrument was calibrated with distilled water before each session.[25] Measurements were expressed as °Brix and recorded in triplicate per sample, with mean values used for statistical analysis.

Image Acquisition and Morphological Analysis
Digital images were acquired at each time interval under standardized conditions:

- Fixed camera distance
- Controlled lighting
- Uniform background contrast
- Images were captured using a high-resolution digital camera and stored in RAW format before processing.

Morphological features were extracted using digital image analysis software. Images were:

- Converted to grayscale
- Binarized using adaptive thresholding
- Processed to remove background noise
- Cropped to isolate tuber surface area
- Surface irregularity patterns were then subjected to fractal analysis.

Fractal Dimension (Df) Analysis
Fractal dimension (Df) was calculated using the box-counting method.[46,47]

The binarized image was overlaid with grids of decreasing box sizes (ε). For each grid size, the number of boxes containing part of the tuber surface (N(ε)) was counted.

Df was calculated as:

$$Df = \lim_{\varepsilon \to 0} \left[\log N(\varepsilon) / \log (1/\varepsilon) \right]$$

Practically, Df was estimated from the slope of the linear regression of log N(ε) versus log (1/ε). Higher Df values indicate increased surface complexity and structural irregularity associated with dehydration-induced epidermal stress.

Climatic Data and Environmental Monitoring
Microclimatic conditions during the experimental period (20–24 October) were obtained from the Copernicus Climate Change Service (C3S) via the Thermal Trace platform.[48]

Universal Thermal Climate Index (UTCI) data were extracted for the exact coordinates of the experimental site. These data, provided by the European Centre for Medium-Range Weather Forecasts (ECMWF) under the Copernicus Programme, ensured validated climatic characterization of solar exposure conditions.[49]

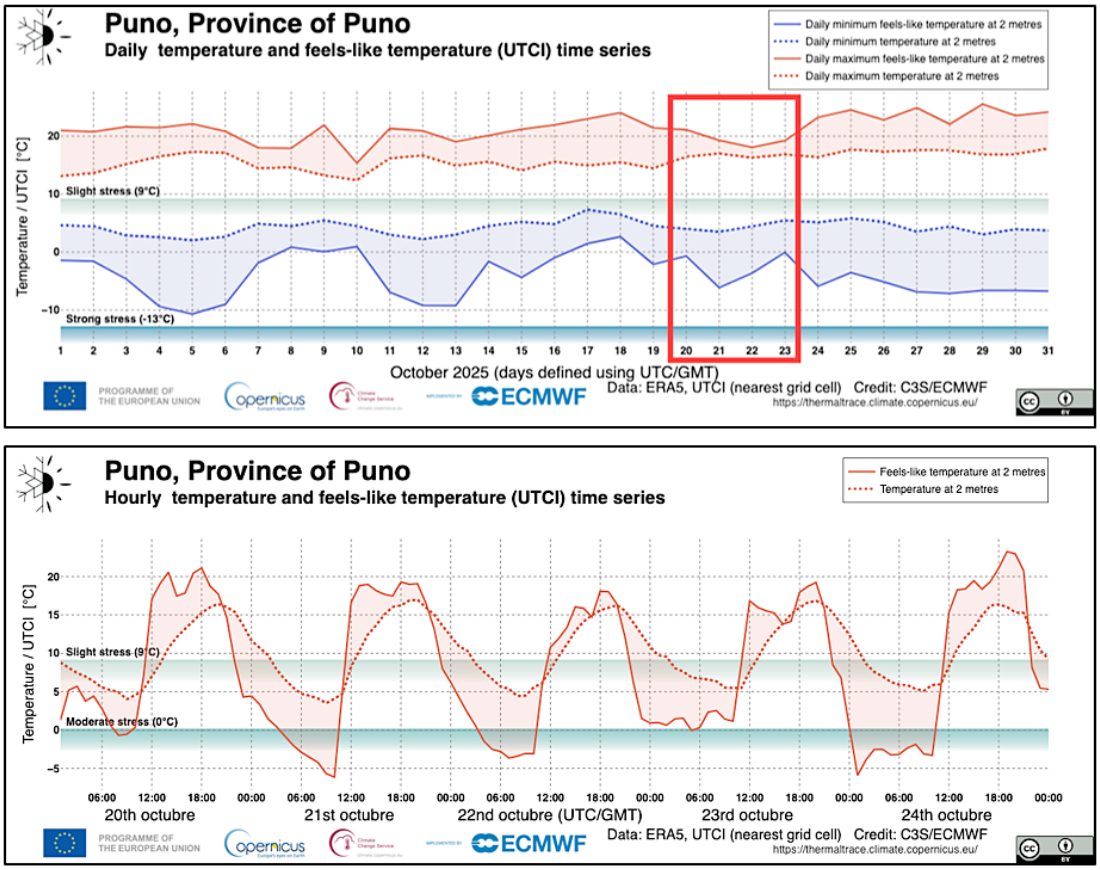

Fig. 2: Daily temperature and UTCI "feels-like" temperature time series for Puno (October 2025), highlighting the experimental period

Statistical Analysis

The study followed a longitudinal repeated-measures design. Time was treated as an ordered factor, and oca variety was considered an independent categorical variable.

Statistical analyses included:

- Descriptive statistics (mean ± standard deviation)
- Pearson correlation coefficients (r) between:
  - °Brix and time
  - °Brix and fractal dimension
  - °Brix and color parameters
- Linear regression analysis to evaluate kinetic trends
- Repeated-measures ANOVA to assess the effect of time and variety
- Post hoc Tukey tests for pairwise comparisons
- Significance level set at $\alpha = 0.05$

All analyses were performed using R version 4.3.2.

Results

Sun-curing induced significant, time-dependent changes in the physicochemical properties of *Oxalis tuberosa* L. across all evaluated ecotypes. The integration of total soluble solids (°Brix) measurements with digital image analysis allowed

objective quantification of sweetening dynamics during natural solar exposure. Descriptive statistics and temporal trends are summarized in Table 1 and Figure 3, respectively.

Table 1: Descriptive statistics of soluble solids content (°Brix) for four Andean *Oxalis tuberosa* L. ecotypes under sun-induced sweetening

Variety	R	Mean R	Mín	Máx	Overall Mean	Overall Median	Mode	SD
Oca INIA 407 K'eny Roja INIA Molina – Salcedo	R1	13.6	6.2	18.3	12.64	12.45	—	3.48
	R2	12.98						
	R3	13.87						
	R4	13.55						
	R5	12.22						
Oca K'eny Roja Sicuani – Cusco	R1	9.73	7.3	11.3	8.74	8.55	8.4	0.97
	R2	8.25						
	R3	8.45						
	R4	9.13						
	R5	8.18						
Oca K'eny Amarilla Capachica	R1	7.23	4.7	10.5	7.3	7.45	—	1.63
	R2	7.65						
	R3	7.03						
	R4	6.18						
	R5	7.82						
Oca K'eny Amarilla Yunguyo	R1	8.47	7.1	10.2	8.63	8.55	8.3	0.87
	R2	8.9						
	R3	8.75						
	R4	8.62						
	R5	8.63						

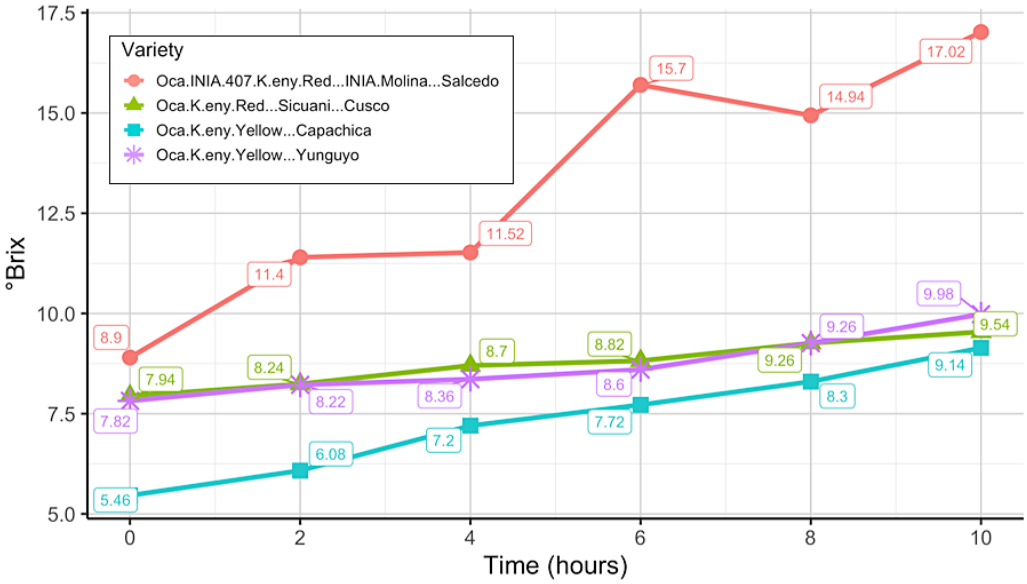

Fig. 3: °Brix evolution in *Oxalis tuberosa* L. ecotypes during sun-induced sweetening behavior of the four evaluated varieties

Two-way ANOVA indicated that both sun-curing time and oca ecotype significantly affected °Brix values ($p < 0.001$), with a significant time × ecotype interaction ($p < 0.01$), demonstrating variety-dependent sweetening.

Red-pigmented ecotypes exhibited higher °Brix values and steeper increases over time. Oca INIA 407 K'eny Roja Molina–Salcedo showed the most pronounced response, increasing from 8.90 °Brix at the initial measurement to 17.02 °Brix after 10 h of exposure. Oca K'eny Roja Sicuani–Cusco also displayed a consistent increase, albeit at a slower rate (7.94–9.54 °Brix). In contrast, yellow ecotypes showed more moderate and homogeneous sweetening patterns. Oca K'eny Amarilla Capachica increased gradually from 5.46 to 9.14 °Brix, while Oca K'eny Amarilla Yunguyo exhibited stable behavior with minimal temporal fluctuations (7.82–9.98 °Brix). Overall, the temporal curves confirm that red ecotypes respond more intensely to solar exposure, whereas yellow ecotypes exhibit smoother sweetening. These differences highlight the influence of varietal pigmentation and genotype-specific metabolic responses on total soluble solids accumulation during traditional Andean sun-curing.

Overall, the combined curves show that red-pigmented ecotypes respond more intensely to solar radiation, reaching higher °Brix concentrations and steeper increases, whereas yellow varieties exhibit slower, smoother, and more controlled sweetening. These patterns indicate that varietal pigmentation and genotype-specific metabolic pathways strongly influence the rate and magnitude of sugar accumulation during traditional Andean sun exposure.

Figure 4 presents the time-based visual evolution of four oca ecotypes, two red and two yellow, over 10 hours after cutting, together with the corresponding changes in °Brix values. All samples show a gradual darkening of the exposed surface and slight structural modifications linked to early oxidative reactions and moisture loss.

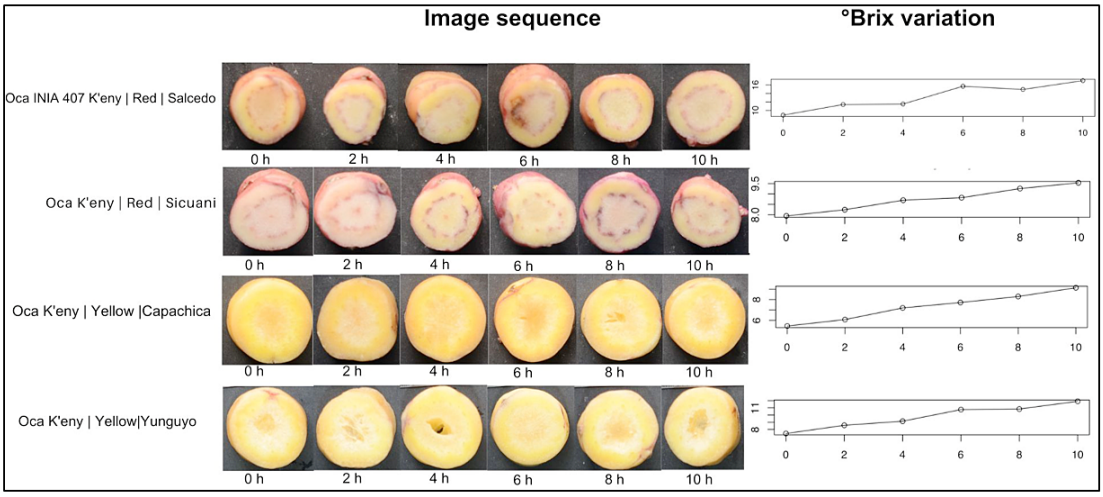

Fig. 4: Visual changes and °Brix variation in four oca ecotypes during 10 hours of post-cut exposure

In parallel, the °Brix curves show a progressive rise in soluble solids, suggesting concentration effects from dehydration and possible enzymatic transformations within the tissue. Overall, the sequence shows how visual deterioration correlates with shifts in sweetness and soluble compound concentration that naturally occur after the tuber's exposure to air.

The following figure illustrates the temporal color progression of four ecotypes, Salcedo, Sicuani, Capachica, and Yunguyo (Figure 5), over a 10-hour post-cut period. Through RGB-based heatmaps and HSV color wheel mapping. All images were acquired under controlled illumination conditions

using a fixed light source and camera settings. Color values were normalized using a reference background to minimize illumination bias prior to RGB–HSV conversion.

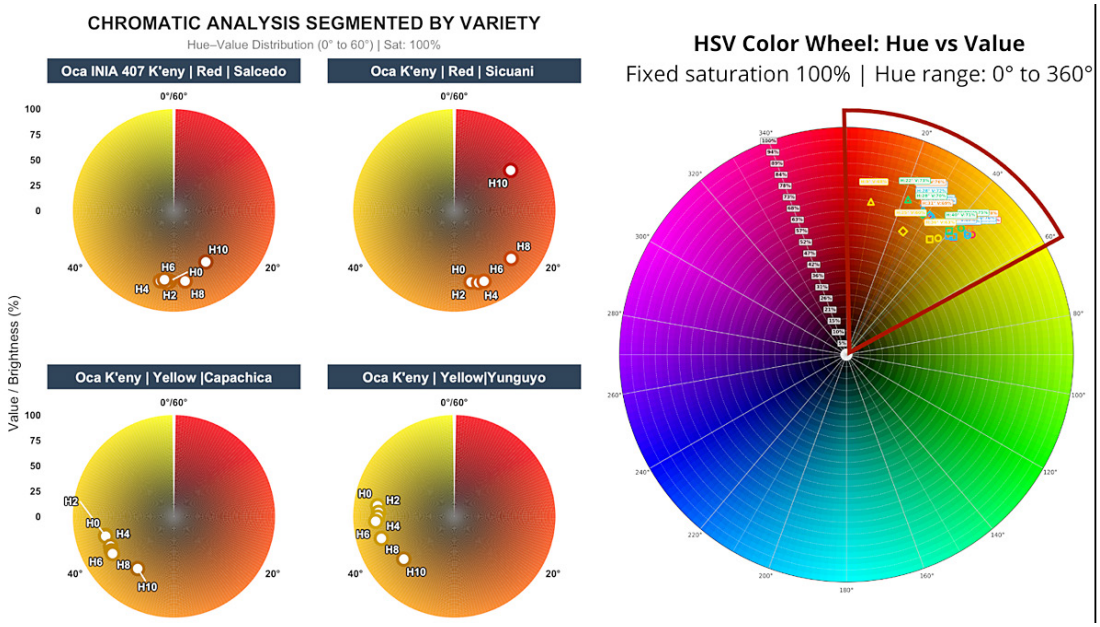

Fig. 5: Temporal color changes in four Oca ecotypes are represented through RGB-based heatmaps

Chromatic analysis in the HSV (Hue-Saturation-Value) space reveals distinct degradation patterns between red and yellow oca ecotypes. Red varieties (V1: Salcedo and V2: Sicuani) exhibited significant instability; most notably, V2 showed a drastic hue shift from 7.8° to 9 °, indicating rapid pigment oxidation toward deeper red-brown tones. Conversely, yellow varieties (V3: Capachica and V4: Yunguyo) demonstrated superior chromatic robustness, maintaining hue values within the 35°- 46° range. Despite differences in stability, all ecotypes showed a marked decline in luminosity (L) by the tenth hour (H10), with values dropping to 59.7%–68.1%.

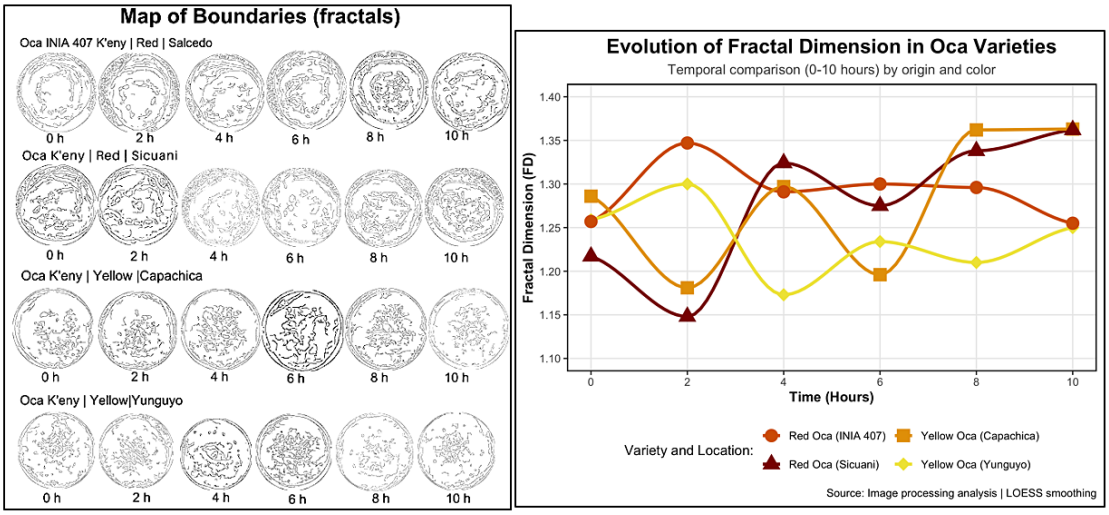

Fig. 6: Fractal dimension dynamics and morphological boundary maps of oca varieties (0–10 h)

The comprehensive analysis of the provided data shows that Fractal Dimension and Brix content (soluble sugars) are distinct quality attributes that are non-linearly correlated across the Oca varieties studied (Figure 6).

While Brix content shows a consistent monotonic upward trend across all varieties over the sampling period (ranging from initial lows of 5.46 to highs of 17.02), consistent with the continuous hydrolysis of starch into sugars during maturity, the Fractal Dimension (Df) exhibits a variety-specific, fluctuating pattern within the range (1.148, 1.363). This fluctuation is particularly noticeable in Roja Molina and Amarilla Yunguyo, which reach their peaks of morphological complexity (approximately 1.300-1.347) early in the process before declining, despite the uninterrupted increase in Brix. The lack of a direct correlation suggests that D, derived via the Box-Counting method, is an extremely sensitive metric for changes in superficial microstructure (roughness, turgidity) induced by initial processing or differential dehydration. In contrast, Brix primarily reflects internal metabolic processes (starch-to-sugar conversion).

The heatmap clearly shows the Pearson correlation coefficients (r) between the Brix index and the Fractal Dimension across four Oca variety-location combinations (Figure 7).

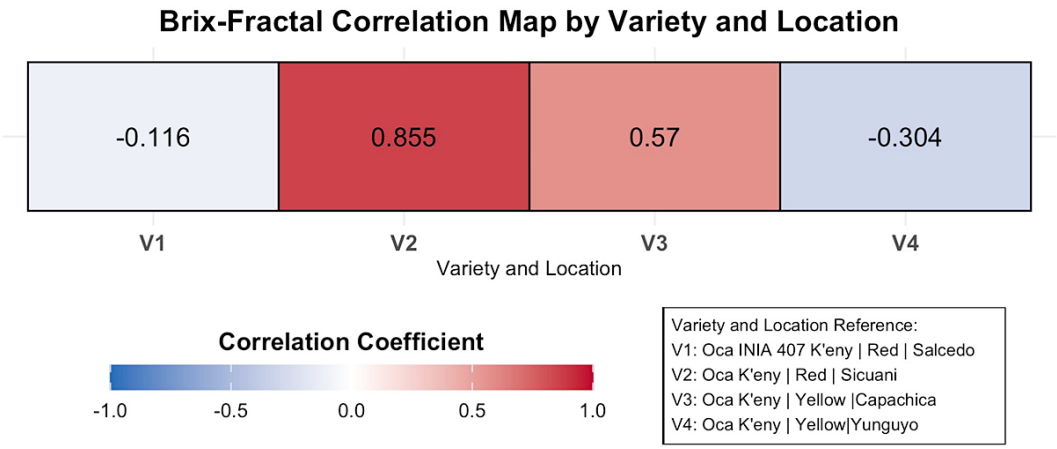

Fig. 7: Brix–Fractal Correlation by Oca Variety and Location

The analysis reveals a diverse set of relationships, with a strong emphasis on positive correlations among specific Andean ecotypes. The most notable result is a robust positive correlation (r = 0.855) for the V2 variety (Oca K'eny Red Sicuani). This highly significant value indicates that, in this ecotype and locality, increases in structural complexity (Fractal Dimension) are strongly and linearly associated with higher sugar content (Brix index), suggesting an optimal structural profile linked to superior quality metrics. A moderately strong positive correlation (r = 0.570) for V3 (Oca K'eny Yellow Capachica) further supports this trend. Conversely, the analysis highlights weak to negligible negative relationships, specifically a weak negative correlation (r = -0.304) for V4 (Oca K'eny Yellow Yunguyo), where increased complexity is slightly linked to reduced sweetness, and a near-zero correlation (r = -0.116) for V1 (Oca INIA 407 K'eny Red Salcedo), demonstrating independence between the two parameters in that combination. Two-way ANOVA revealed that both sun-curing time and oca variety had a significant effect on °Brix values ($p < 0.001$), with a significant time × variety interaction ($p < 0.01$), indicating varietal differences in sweetening.

Discussion

Castañeta *et al.*,[13] demonstrated that sun exposure in *Oxalis tuberosa* L. induces significant physicochemical changes, primarily driven by moisture loss and increased soluble solid concentration rather than uniform biochemical transformation. This pattern aligns with the moderate, variety-dependent correlations between °Brix and fractal parameters observed in this study, indicating that sweetening during asoleado follows distinct

trajectories depending on genotype and growing location.[6,33] These correlations describe temporal co-evolution rather than direct causality. The two-way ANOVA results confirm that exposure time and oca ecotype significantly affect °Brix values ($p < 0.001$), with a significant time × ecotype interaction ($p < 0.01$), demonstrating that red-pigmented varieties respond more intensely to solar exposure than yellow varieties, suggesting intrinsic differences in starch hydrolysis rates or sugar precursor availability.

From a structural perspective, Peleg,[25] and García-Armenta and Gutiérrez-López,[17] established that fractal dimension robustly describes surface complexity arising from dehydration-induced microstructural rearrangements. The contrasting correlations between °Brix and fractal dimension across varieties suggest that physical surface evolution is not linearly coupled to sugar concentration, consistent with previous findings in food systems undergoing drying.[19,20,27] The strong positive correlation between °Brix and exposure time (r = 0.88–0.94) provides quantitative validation of traditional sun-curing practices, indicating that exposure duration can serve as a reliable predictor of soluble solid content, thereby enabling standardization of the sweetening process for agroindustrial applications

Regarding visual attributes, Pedreschi *et al*.,[47] highlighted that color changes during dehydration are strongly linked to surface irregularities and oxidation phenomena rather than to soluble solid content alone. This explains the weak association among color, °Brix, and fractal behavior detected here, reinforcing the notion that color degradation evolves semi-independently under solar exposure.[49] The moderate-to-strong correlations between color and °Brix (r = 0.76–0.85), though statistically significant, are notably weaker than the time-°Brix relationship, reflecting the distinct kinetics of enzymatic browning and pigment oxidation, which are accelerated by solar exposure but not directly driven by sugar accumulation.

Overall, in agreement with Campoverde Caicedo and Meneses Quelal,[45] the results confirm that postharvest responses in oca are genotype-dependent and multidimensional. Integrating °Brix, fractal analysis, and color metrics provides a more comprehensive framework for characterizing sweetening and structural changes during traditional sun-drying processes.[45]

Conclusion

Traditional sun-curing under high-altitude Andean conditions produced significant, time-dependent increases in total soluble solids (°Brix) in *Oxalis tuberosa* L., with clear differences among ecotypes. Red-pigmented varieties exhibited faster and higher °Brix accumulation than yellow ecotypes, confirming genotype-dependent sweetening during solar exposure. The strong positive correlation between exposure time and °Brix (r = 0.88–0.94) validates the empirical knowledge of Andean farmers and demonstrates that sweetening follows predictable kinetic patterns. Surface morphological analysis revealed dynamic and variety-specific changes in fractal dimension, with a non-linear relationship to °Brix that varies by ecotype and locality. Fractal dimension should be interpreted as a complementary descriptor of post-harvest surface dynamics rather than a universal proxy for sweetness. The integration of digital image analysis, fractal geometry, and physicochemical measurements provides an objective framework for characterizing traditional sun-curing processes. This multiparametric approach enables data-driven decision-making for optimizing post-harvest handling and improving quality consistency. The genotype-dependent responses suggest that breeding programs could prioritize oca varieties with superior sweetening kinetics, enhancing competitiveness in regional and international markets. This study is limited by evaluation of a single curing duration (10 hours), a restricted number of ecotypes (four varieties), and field-based environmental variability (cloud cover, wind, microclimate). The study did not include enzymatic assays or detailed sugar-profile analyses. Future research should incorporate controlled radiation conditions, expanded varietal sampling, enzymatic and sugar-profile analyses, longitudinal tracking of individual tubers, and integration of genomic data to refine morphological indicators as decision-support tools in post-harvest management.

Acknowledgement

The authors gratefully acknowledge the support of the Universidad Nacional del Altiplano (Puno, Peru) for providing the facilities, institutional support, and

resources necessary for the development of this research. Their collaboration was essential for the successful execution of the experimental and analytical procedures.

Funding Sources
The authors received no financial support for the research, authorship, and/or publication of this article.

Conflict of Interest
The authors do not have any conflicts of interest.

Data Availability Statement
The manuscript incorporates all datasets generated or analyzed throughout this study.

Ethics Statement
This research did not involve human participants, animal subjects, or any material that requires ethical approval.

Informed Consent Statement
This study did not involve human participants, and therefore, informed consent was not required.

Clinical Trial Registration
This research does not involve any clinical trials.

Permission to Reproduce Material from Other Sources
Not Applicable.

Author Contributions
- **Roenfi Guerra Lima:** Conceptualization, Methodology, Formal Analysis, Software, Data Curation, Sources Recollection.
- **Edward Torres Cruz:** Conceptualization, Methodology, Formal Analysis, Writing Original Draft Preparation, Visualization, Validation.
- **Fred Torres Cruz:** Validation, Data Curation, Graphics drawing.
- **Wenceslao T. Medina:** Validation, Writing Original Draft Preparation.
- **Nury Yaneth Mayta Barrios:** Conceptualization, Methodology, Formal Analysis.

References

1. Llaja-Zuta E, Fernández-Poquioma DM, Añazco-Urbina B, Hernández-Amasifuen AD, Condori-Apfata JA. In vitro micropropagation of oca (*Oxalis tuberosa* Mol.): an important plant genetic resource from the high Andean region. *Plants.* 2025;15(1):62. doi:10.3390/plants15010062
2. Loyo-Trujillo NA, Mendoza-López MR, Guzmán-Gerónimo RI, *et al*. Impact of the physical modification of starch (*Oxalis tuberosa*) in a low-fat snack by hot air frying, a sustainable process. *Foods.* 2025;14(16):2909. doi:10.3390/foods14162909
3. Sperling CR, King SR. Advances in new crops. In: Janick J, Simon JE, eds. Proceedings of the First National Symposium on New Crops: Research, Development, Economics. Portland, OR: Timber Press; 1990:428-435.
4. Hermann M, Heller J. Andean roots and tubers: ahipa, arracacha, maca and yacon. In: Hermann M, Heller J, eds. Promoting the Conservation and Use of Underutilized and Neglected Crops. Vol 21. Rome: Institute of Plant Genetics and Crop Plant Research; 1997:5-12.
5. Torres Cruz E, Cahuana Lipa R, Machaca Mamani JC, *et al*. Effect of protein-based edible coatings on the preservation and shelf life of strawberries (Fragaria × ananassa). *Nutr Clin Diet Hosp*. 2025;45(4):202-209. doi:10.12873/454torres
6. Elewa MS, El-Saady G, Ibrahim K, Tawfek M, Elhossieny H. A novel method for Brix measuring in raw sugar solution. *Egypt Sugar J*. 2020. doi:10.21608/ESUGJ.2020.209517
7. Scapin T, Fernandes AC, Curioni CC, *et al*. Influence of sugar label formats on consumer understanding and amount of sugar in food choices: a systematic review and meta-analysis. *Nutr Rev.* 2021. doi:10.1093/nutrit/nuaa108

8. Melín P, Castillo O. An adaptive model-based neuro-fuzzy-fractal controller for biochemical reactors in the food industry. In: Proceedings of the IEEE International Joint Conference on Neural Networks. *IEEE*; 1998. doi:10.1109/IJCNN.1998.682245
9. de Lima R, Marreiros G, Fdez-Riverola F, Vicente H, Neves J. Non-ergodic theory vs fractal geometry in organizational learning and dynamic skills at a healthcare food catering service. In: Lecture Notes in Networks and Systems. Springer; 2024. doi:10.1007/978-3-031-80946-0_19
10. Caballero D, Caro A, Ávila M, Rodríguez PG, Antequera T, Palacios TP. New fractal features and data mining to determine food quality based on MRI. *IEEE Lat Am Trans.* 2017. doi:10.1109/TLA.2017.8015085
11. Barletta BJ, Barbosa-Cánovas GV. Fractal analysis to characterize ruggedness changes in tapped agglomerated food powders. *J Food Sci.* 1993. doi:10.1111/j.1365-2621.1993.tb06105.x
12. Quevedo R, Carlos LG, Aguilera JM, Cadoche L. Description of food surfaces and microstructural changes using fractal image texture analysis. *J Food Eng*. 2002;53(4):361-371. doi:10.1016/S0260-8774(01)00177-7
13. Castañeta G, Castañeta R, Peñarrieta JM. Cambios fisicoquímicos por exposición a la radiación solar en tubérculos de *Oxalis tuberosa* "oca" cultivados en Bolivia. *Rev Boliv Quim.* 2022;39(2). doi:10.34098/2078-3949.39.2.3
14. Hagiwara T, Wang H, Suzuki T, Takai R. Fractal analysis of ice crystals in frozen food. *J Agric Food Chem.* 2002;50(11):3085-3089. doi:10.1021/jf011240g
15. Morandini L, Buda A, Fraternali P. Geospatial artificial intelligence for solid waste recognition from UAV imagery. *E3S Web Conf*. 2025. doi:10.1051/e3sconf/202564301004
16. Rastegari M, Ordonez V, Redmon J, Farhadi A. XNOR-Net: ImageNet classification using binary convolutional neural networks. In: European Conference on Computer Vision (ECCV). Springer; 2016. doi:10.1007/978-3-319-46493-0_32
17. García-Armenta E, Gutiérrez-López GF. Fractal microstructure of foods. Food Eng Rev. 2022. doi:10.1007/s12393-021-09302-y
18. Al-Dairi M, Pathare PB, Al-Yahyai R, Jayasuriya H, Al-Attabi Z. Banana fruit bruise detection using fractal dimension-based image processing. *Food Chem.* 2024;455:139812. doi:10.1016/j.foodchem.2024.139812
19. Kerdpiboon S, Devahastin S. Fractal characterization of some physical properties of a food product under various drying conditions. *Dry Technol*. 2007. doi:10.1080/07373930601160973
20. Sampurno J. Analisis fraktal untuk identifikasi kadar gula rambutan dengan metode box-counting. 2018;6(2):57-60.
21. Cruz G, Ribotta PD, Ferrero C, Iturriaga L. Physicochemical and rheological characterization of Andean tuber starches: potato, oca and papalisa. *Starch/Stärke.* 2016. doi:10.1002/star.201600103
22. Santacruz S. Characterisation of starches isolated from Arracacha xanthorriza, Canna edulis and *Oxalis tuberosa*. PhD thesis. University of Nottingham; 2004.
23. Badarou ASD, Lagnika C, Hounhouigan HM, *et al*. Migration of antimony and phthalate esters from plastic food packaging: a systematic review. *Curr Res Nutr Food Sci.* 2025;13(3):1079-1105. doi:10.12944/crnfsj.13.3.4
24. Savage GP, Mason SL, Vanhanen L. The effect of storage on the oxalate content of New Zealand grown oca. *Int J Food Sci Technol.* 2008;43(12):2130-2133. doi:10.1111/j.1365-2621.2008.01807.x
25. Peleg M. Fractals and foods. *Crit Rev Food Sci Nutr.* 1992;32(4):363-369. doi:10.1080/10408399309527617
26. Andoyo R, Lestari VD, Mardawati E, Nurhadi B. Fractal dimension analysis of texture formation of whey protein-based foods. *Int J Food Sci.* 2018. doi:10.1155/2018/7673259
27. Kerdpiboon S, Devahastin S, Kerr WL. Comparative fractal characterization of physical changes of different food products during drying. *J Food Eng.* 2007. doi:10.1016/j.*jfoodeng.*2007.03.039
28. Mostofa M, Roy TS, Chakraborty R, Ferdous J, Nowroz F, Noor R. Effect of vermicompost and tuber size on total soluble solids and sucrose of potato during storage. *Azarian J Agric.* 2019. doi:10.29252/azarinj.008
29. Lura-Murillo RP, Torres-Cruz F, Suaquita

JRH, Auquitias-Condori GM, Herrera-Urtiaga AP. Multi-platform framework for pattern and image processing. In: Lecture Notes in Networks and Systems. 2023;669:501-509. doi:10.1007/978-3-031-29860-8_51

30. Bradbury EJ, Emshwiller E. The role of organic acids in the domestication of *Oxalis tuberosa*: a model for studying domestication resulting in opposing crop phenotypes. 2010.
31. Castañeta G, Miranda-Flores D, Bustos AS, *et al*. Influence of sunlight exposure and traditional dehydration on chemical and nutritional properties of *Oxalis tuberosa*. *Plant Foods Hum Nutr.* 2025;80(2):91. doi:10.1007/s11130-025-01330-x
32. King SR, Gershoff SN. Nutritional evaluation of three underexploited Andean tubers: *Oxalis tuberosa*, Ullucus tuberosus and Tropaeolum tuberosum.
33. Jaywant SA, Singh H, Arif KM. Sensors and instruments for Brix measurement: a review. *Sensors*. 2022;22:2290. doi:10.3390/s22062290
34. Hosseini M, Bari MR, Alizadeh M. Production of synbiotic juice: effect of pH, Brix, formalin index and rheological properties. *AYERS.* 2016.
35. Areche FO, Huayhua LLA, Huamán JT. Efecto del tiempo y temperatura en la deshidratación de oca mediante lecho fluidizado para obtención de harina. *Rev Alfa.* 2020. doi:10.33996/revistaalfa.v4i12.84
36. Pissard A, Arbizu C, Ghislain M, *et al*. Congruence between morphological and molecular markers in *Oxalis tuberosa*. *Genetica*. 2008;132(1):71-85. doi:10.1007/s10709-007-9150-9
37. Estrada-Fernández AG, Dorantes-Bautista G, Román-Guerrero A, *et al*. Modification of *Oxalis tuberosa* starch with OSA and application in Pickering emulsions. *J Food Sci Technol.* 2021. doi:10.1007/s13197-020-04790-y
38. Morales NXC, Gómez KYV, Schweiggert RM, Delgado GTC. Stabilisation of betalains extracted from cactus pear using oca starch. *Food Sci Technol Int.* 2021. doi:10.1177/1082013220963973
39. Núñez-Bretón LC, Cruz-Rodríguez LC, Tzompole-Colohua ML, *et al*. Physicochemical characterization of Mexican *Oxalis tuberosa* starch modified by cross-linking. *J Food Meas Charact.* 2019. doi:10.1007/s11694-019-00207-3
40. Jiménez-Guzmán J, Morales-Morales TY, Buendía-Hernández TG, *et al*. Influence of drying method on microstructural properties of *Oxalis tuberosa* starch. *J Food Meas Charact.* 2022. doi:10.1007/s11694-022-01465-4
41. Peralta EV. Determinación de parámetros tecnológicos para la elaboración de mermelada a partir de oca y manzana. Thesis. 2012.
42. Liu T, Burritt DJ, Eyres GT, Oey I. Pulsed electric field processing reduces oxalate content of oca tubers. *Food Chem.* 2018;245:1111-1117. doi:10.1016/j.foodchem.2017.11.085
43. Castro-Mendoza MP, Palma-Rodríguez HM, Heredia-Olea E, *et al*. Characterization of a mixture of oca and oat extrudate flours. *J Food Qual.* 2019. doi:10.1155/2019/1238562
44. Vera W, Quevedo-Olaya JL, Minchán-Velayarce H, *et al*. Impact of the physical modification of starch (*Oxalis tuberosa*) in a low-fat snack by hot air frying. *Foods.* 2025;14(16):2909. doi:10.3390/foods14162909
45. Campoverde Caicedo A, Meneses Quelal O. Challenges and opportunities of *Oxalis tuberosa* cultivation from an Andean agroecological perspective. *Sustainability.* 2025;17(14):6470. doi:10.3390/su17146470
46. Joshi BL, Beccard S, Vilgis TA. Fractals in crystallizing food systems. *Curr Opin Food Sci.* 2018;21:34-39. doi:10.1016/j.cofs.2018.05.009
47. Pedreschi F, Aguilera JM, Brown C. Characterization of food surfaces using scale-sensitive fractal analysis. *J Food Process Eng.* 2000. doi:10.1111/j.1745-4530.2000.tb00507.x
48. Copernicus Health Hub. Thermal trace: tracking heat and cold stress worldwide. https://health.hub.copernicus.eu/thermal-trace-tracking-heat-and-cold-stress-worldwide. Accessed January 9, 2026.
49. European Centre for Medium-Range Weather Forecasts. Medium-range forecasts. https://www.ecmwf.int/en/forecasts/documentation-and-support/medium-range-forecasts. Accessed January 9, 2026.